Unfolding cross-linkers as rheology regulators in F-actin networks

B. A. DiDonna
Institute for Mathematics and its Applications, University of Minnesota, Minneapolis, Minnesota 55455-0436, USA

Alex J. Levine
Department of Chemistry and Biochemistry, and the California Nanosystems Institute University of California, Los Angeles, California 90095, USA

(Received 10 August 2006; revised manuscript received 20 December 2006; published 16 April 2007)

We report on the nonlinear mechanical properties of a statistically homogeneous, isotropic semiflexible network cross-linked by polymers containing numerous small unfolding domains, such as the ubiquitous F-actin cross-linker filamin. We show that the inclusion of such proteins has a dramatic effect on the large strain behavior of the network. Beyond a strain threshold, which depends on network density, the unfolding of protein domains leads to bulk shear softening. Past this critical strain, the network spontaneously organizes itself so that an appreciable fraction of the filamin cross-linkers are at the threshold of domain unfolding. We discuss via a simple mean-field model the cause of this network organization and suggest that it may be the source of power-law relaxation observed in *in vitro* and in intracellular microrheology experiments. We present data which fully justify our model for a simplified network architecture.

DOI: 10.1103/PhysRevE.75.041909 PACS number(s): 87.16.Ka, 82.35.Rs, 62.20.Dc

I. INTRODUCTION

The cytoskeleton of eukaryotic cells can be described as a biopolymer gel or cross-linked network [1–3]. The principal constituent of the cytoskeleton is a stiff protein aggregate, F-actin, that is cross-linked densely on the scale of its own thermal persistence length. In this sense the mesoscale structure of this biopolymer network differs substantially from that of synthetic polymer gels [4], which may be thought of as interconnected random walks. This realization of the profound differences in mesoscale structure between the cytoskeleton, a prototypical semiflexible filament network, and flexible polymer gels calls into question the application of standard rubber elasticity theory to describe the mechanics of semiflexible networks.

A number of researchers have begun to explore the quantitative relation between the novel microstructure of semiflexible gels and their observed mechanical properties [5–7]. More recently, it has been proposed that, due to their different architecture, these semiflexible gels have macroscopic linear moduli that are generically more sensitive to their chemical composition [9–14] than traditional flexible gels. Their response to point forces over mesoscopic distances is much more complex than suggested by the predictions of continuum elasticity [15]. In addition, they exhibit a highly tunable (through network microstructure) nonlinear response to stress [16].

Understanding the biophysical properties of the cytoskeleton demands a closer examination not only of the material properties of generic semiflexible networks, but also of the chemical heterogeneity of the physiological cytoskeleton. Until recently, numerical and theoretical modeling of the relationship between the network architecture on the mesoscale and the long-length scale mechanical properties of these gels has focused exclusively on semiflexibility of the filaments [17] while ignoring the details of the chemical agents which cross-link them. Recent *in vitro* experiments, however, have shown that the nanoscale mechanics of the physiologically ubiquitous cross-linking proteins have a significant effect on the mechanics of cross-linked F-actin networks [18]. One particularly interesting class of cross-linkers from the standpoint of network mechanics are those that contain unfolding domains such as α-actinin [19,20] and filamin [21,22]. Such cross-linkers have protein domains along their backbone that unfold reversibly at a critical pulling force. It is still a matter of debate what the function of these domains may be, but one may speculate that, by exposing new chemical groups in the unfolded domains, cross-linking agents such as filamin may play a role in transducing local network strain into biochemical signals.

In this paper we investigate the purely mechanical effect of cross-linkers which have unfolding domains. The mechanical effect of domain unfolding occurs only at some finite applied stress, so the effect we wish to study is evident only in the nonlinear elastic response of the material observed under finite strain conditions. In this aspect the present work differs from much of the recent theoretical research on semiflexible network mechanics that focused on the linear response regime.

We demonstrate two effects that the inclusion of unfolding cross-linkers has on the elastic properties of an otherwise generic semiflexible network. Firstly, since the cross-linkers can only sustain a finite maximum tensile stress before unfolding, their inclusion leads to shear softening of the network at large strain. Secondly, past the onset of shear softening the network spontaneously organizes so that the population of cross-links at given tension grows exponentially or faster up to the unfolding force of the domains. Thus, at moderate applied stresses the system appears to adjust its mechanical properties so as to achieve a strain state in which a significant fraction of its cross-linkers are poised at the unbinding transition of their internal domains. We refer to such cross-linkers as being in a critical state. In a thermalized system, the rapidly rising population of cross-links weighted towards the unfolding force would yield a fragile state of the material characterized by a broad, continuous

distribution of relaxation time scales via thermally excited subcritical cross-link unfolding. This thermally excited unfolding may account for the broad, i.e., power law distribution of stress relaxation times that has been observed in *in vivo* experiments [23–27] and has been termed soft-glassy rheology (SGR) [28]. While in our purely mechanical model this fragile state, in which critical cross-linkers predominate, comes about as a consequence of applied stress, an *in vivo* network built with unfolding cross-linkers may generically evolve into this high susceptibility state under the action of internal molecular motors (e.g., myosin—not considered in our model). The necessity of applied stress to enter this fragile state in absence of molecular motors appears to be consistent with the recent finding that prestress is necessary to replicate *in vivo* rheology measurements in artificially synthesized actin-filamin networks [18].

The remainder of this article is arranged as follows. In Sec. II we present a simple mean-field theory for the mechanical effects of cross-linkers with unfolding domains. In Sec. III we discuss our numerical model used to study the strain response of an F-actin network with unfolding cross-links. Sections II and III reiterate material presented in our initial article on this subject [29], while the following sections go beyond the preliminary analysis presented therein. We present the results of this modeling in Sec. IV and compare them to our theory. Finally we conclude in Sec. V where we discuss the generality of our results and place them in the broader context of the mechanics of semiflexible gels and the modeling of the cytoskeleton in particular.

II. THEORY

We now consider how the incorporation of cross-linkers with unfolding immunoglobin domains will affect the equilibrium states of a random semiflexible filament network. The elasticity of the unfolding cross-linkers is highly nonlinear due to the presence of the many identical folded protein domains (24 in the case of filamin). It is observed at large tensile forces ($\sim$100 pN) that one of these domains will open, increasing the contour length of the molecule by about $\sim$20 nm and thereby relaxing the stress in the system.

As a simple approximation, we model the force extension curve of a single cross-linker as a sawtooth. Each branch of the sawtooth represents the entropic elasticity of a cross-linker with a fixed number of unfolded domains. For simplicity, we take the additional contour length generated during any unfolding event l_f to be a constant and the force-extension relation on each branch of the sawtooth to be linear with spring constant k_f. Thus the maximum force on each branch of the sawtooth $k_f l_f$ corresponds to the critical unfolding force of a domain. We also neglect the rate dependence of this unfolding force [30] that is found in nonequilibrium unfolding dynamics. We refer to this simplified mechanical model of the physiological cross-linkers as a sawtooth cross-linker. Clearly any biopolymer cross-linker that has multiple unfolding domains that are accessible at physiologically relevant tensions will act in this manner. We expect the results presented below to apply to a network cross-linked by any molecule of this class.

We now consider the effects of such sawtooth cross-linkers on the zero frequency mechanics of an elastic network cross-linked by such agents. In the following we show that the considerations of force balance alone allow us to relate the distribution of sawtooth cross-linker extensions modulo the sawtooth length to the, as yet, unknown distribution of local network compliances in the randomly cross-linked network.

Imagine the equilibrium state of an individual pulled sawtooth cross-linker and the region of network surrounding it both before and after a single unfolding event. We assume that for the relatively short sawtooth length l_f found in physiological networks, the response to one unfolding is in the linear regime of the surrounding network. We model the surrounding effective medium as a single harmonic spring with spring constant k sampled from some statistical distribution $P_K(k)$ which encapsulates the differing local environments around each cross-link. Reflecting the network structure, the cross-linker is connected in series with the effective network spring. We first set the total strain on the two springs in series (by fixing their combined length) so that the cross-link is poised at the maximum extension of its current sawtooth branch. Then we consider an infinitesimal increase in the total extension which drives the unfolding of one more protein domain.

Before the unfolding event the two springs are in force balance at the top of the previous sawtooth branch, so that $k_f l_f = kx$, where x represents the extension of the medium spring. After the unfolding, the system achieves force balance on the next branch of the sawtooth force-extension curve so that the extension of the cross-linker is now increased by $l_f - d$ while the extension of the medium spring is decreased to $x-(l_f-d)$. Force balance requires that d, the distance between the current extension of the cross-linker and the edge of the next sawtooth, is given by $d(k)=kl_f/(k+k_f)$. In other words, the combined system once equilibrated with the cross-linker at its maximal force is now equilibrated with that cross-linker on its next sawtooth branch at a smaller force. The strain in the surrounding medium has also decreased due to the extension of one more protein domain.

To maintain force balance, the cross-linker cannot relax its length more than l_f-d. Upon further extension the cross-linker will only stretch more until another domain unbinds. Thus in steady-state the sawtooth cross-linker will evenly sample all extensions (modulo l_f) between $l_f-d(k)$ and l_f. For a given value of the spring constant of the medium we expect that the extensions (modulo l_f) of the sawtooth cross-linkers x_f to be uniformly distributed between the bounds given above. This distribution can be written as

$$P(x_f,k) = \frac{1}{d(k)}\Theta(x_f - [l_f - d(k)]), \tag{1}$$

where Θ is a step function. Integrating over the spring constant distribution $P_K(k)$, we write the probability of finding a given cross-linker length (modulo l_f) x_f:

$$P(x_f) = \int_{k_f[(l_f-x_f)/x_f]}^{\infty} \frac{k_{\text{eff}}+k_f}{l_f k_{\text{eff}}} P_K(k_{\text{eff}})dk_{\text{eff}}. \tag{2}$$

The step function fixes the lower limit on the k integral.

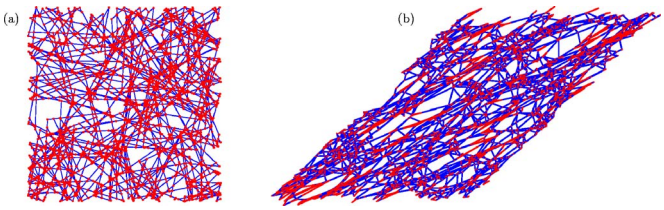

FIG. 1. (Color online) Model network showing the F-actin filaments in blue and the sawtooth cross-linking agents in red. (a) Unstrained. (b) 100% shear.

There are several important observations to make concerning Eq. (2). First we have treated the unfolding events as being uncorrelated. In this mean field model we have ignored the effect of additional unfolding events in the surrounding medium. This simplification allows us to treat the surrounding network as a linear elastic element with an undetermined spring constant k. We will test this assumption by comparing the predicted relation (2) to our numerical data. From this equation we note that the appearance of an exponential peak in the extension distribution $P(x_f,k)$ requires a nontrivial structure for the distribution of local spring constants $P_K(k)$. This distribution itself depends on the random connectivity and material distribution of the network. Below we will examine this distribution in some detail numerically and we defer speculations about its form for Sec. IV B, where we discuss our numerical results.

A second feature of Eq. (2) is that it can be rescaled by l_f^{-1} in such a way that the dimensionless length distribution $P(x_f/l_f)$ is completely independent of the sawtooth length l_f. Thus the distribution $P(x_f/l_f)$ modulo 1 depends only on k_f and $P_K(k)$. We now turn to a discussion of the numerical model we used to study random networks with unfolding cross-links.

III. NUMERICAL MODEL

We employ a simple simulational model of a statistically homogeneous, isotropic network of semiflexible filaments in two dimensions. These networks are formed in a manner identical to that of Head *et al.* [9,11,12], i.e., by placing straight rods of a fixed length at random positions and orientations in a box with periodic boundaries. At points where two rods intersect a node is added to each rod and a cross-linker is added connecting the nodes. The cross-linkers have zero rest length. Rods are added until the average number of cross-links per rod reaches a target value that we use to parameterize the network density. A model network constructed by the procedure described above is shown in Fig. 1. The sections of rod between nodes are modeled as linear springs with fixed elastic constant per unit length of rod. The cross-linkers exert no constraint torques at the nodes so that the rods are free to bend there with no energy cost. We write the Hamiltonian for each filament as

$$\mathcal{H} = \frac{1}{2}\mu \int \left(\frac{dl(s)}{ds}\right)^2 ds, \tag{3}$$

where $dl(s)/ds$ gives the strain or relative change in local contour length, and μ is the Young's modulus of the filament (essentially a spring constant normalized to 1/[length]).

We found that all numerical minimization routines we tried failed to converge in the nonlinear large shear regime when the energetics of filament bending were added to our simulational model. This is due to the large distribution of length scales in the random network, and the resulting poorly conditioned Jacobian. At the same time, the nonlinear behavior of semiflexible networks with freely rotating cross-links has been shown to be dominated by semiflexible filament stretching instead of bending [17]. We therefore omit bending energies from our model. This omission allows for significant gains in computational efficiency and leads to negligible errors in the high-strain state, on which we focus. The effect of this approximation on our results will be discussed where appropriate.

Similarly, we anticipate that the results derived here are essentially independent of network dimensionality since network connectivity, not the dimensionality of the space in which the network is embedded, should control the collective mechanical properties of the system. Based on the justification given in Sec. II, we model the unfolding crosslinkers as non-linear springs with a sawtooth force extension law. Once again, the sawtooth branches have linear spring constant k_f and length l_f. Though the physiological filament cross-linkers have a finite number of unfolding domains (24), we will let our simulated sawtooth force extension curve have an infinite number of branches.

The network is sheared using Lees-Edwards boundary conditions (by adding a constant horizontal offset to filaments that crossed the top and bottom boundaries) as shown in Fig. 1(b). At the beginning of each strain step all nodes are moved affinely, then the node positions are relaxed through a conjugate gradient routine to a point of local force equilibrium. Since the cross-linker force extension curve is a sawtooth, there are many possible equilibrium states of the network. We wish to consider the adiabatic, history dependent states of a strained network, which would in principle require us to use strain steps resulting in displacements smaller than the sawtooth length l_f so that mechanical equilibrium is achieved in the earliest possible branch. To save computational time we use a two step equilibration procedure, which finds a state close to adiabatic state, but allows for large strain steps. In the first equilibration step, we replace the sawtooth force law for all cross-linkers by the following force law:

$$\mathbf{f} = \begin{cases} k_f \mathbf{x}, & |\mathbf{x}| < l_f, \\ k_f l_f, & |\mathbf{x}| \geqslant l_f. \end{cases} \tag{4}$$

Thus, beyond the first sawtooth length, a cross-linking molecule exerts a constant contractile force of magnitude $k_f l_f$. The combined network of linear elastic rods and constant force cross-links is equilibrated. Finally, we reimpose a sawtooth force law for the cross-linkers and equilibrated the network a second time. Assuming all cross-links act independently as the network relaxes during this final equilibration step, the force on the cross-link must be less than $k_f l_f$, so the cross-link will stay on the same sawtooth branch. Since the rest of the network was originally equilibrated at the critical

TABLE I. Scaled values of simulation parameters. The scaled Ig domain length and cross-link separation were taken from the literature [31,32], and were the basis of the chosen simulational values. The total filament length derives from the cross-link separation and the decision to use 30 cross-links per filament on average. This value is consistent with physiological values. The simulational value of spring ratios were chosen to be broader than the typical physiological ratios, so as to capture all possible regimes.

Parameter	Symbol	Sim units	Scaled units
Ig domain length	l_f	6.5×10^{-4}	20 nm
cross-link separation	l_c	6.6×10^{-3}	0.2 μm
filament length	l_R	0.2	6 μm
spring ratio	$k_f/\langle k_R\rangle$	0.06–66	0.4–7

pulling force, the sawtooth force law could not have reached force equilibrium on any earlier sawtooth branch. In practice, collective relaxations of the network push individual cross-links onto different sawtooth branches in this final step. However, we found that for a variety of strain step sizes the quantitative behavior discussed in the results section was identical. This numerical technique reduced the required computational time by a factor of ten or more, allowing us to simulate up to six realizations of random networks, each with an average of 1100 filaments and 16 500 crosslinks, for every set of material values in this study. With this technique, we were able to arrive at statistically meaningful results in a reasonable number of computer processor hours.

IV. SIMULATION RESULTS

The numerical values for all parameters in the simulation, as well as their corresponding physical values, are presented in Table I. We present data for networks with a filament density such that there are on average 30 cross-links per filament. The filaments have a unique length of $l_R=0.2$ measured in units of the length of the unstrained, square simulation box. This gives an average cross-link separation of $l_c \approx 6.6\times10^{-3}$ in simulation units. For these values we find negligible system-size effects. The other length scale in the system is l_f, the length of the sawtooth in our approximate form of the cross-linker force-extension relation. We found that for $l_R/l_c \gtrsim 15$ and l_f/l_c constant, the network behavior is independent of l_R. The distance between cross-links in physiological F-actin networks has been quoted as $l_c=0.2$ μm [31]. For Filamin cross-links each unfolding domain adds $l_f=21$ nm of length [32]. Thus the physiological ratio of sawtooth length to cross-link separation is $l_f/l_c=0.1$. We expect this ratio to be similar for all domain-unfolding cross-linkers. To explore the dependence of our results on this ratio and thus on the particular type of sawtooth cross-linker, we present data for $l_f/l_c\approx0.1$ and $l_f/l_c\approx0.02$ (respectively, we used $l_f=6.5\times10^{-4}$ and $l_f=1.3\times10^{-4}$ in simulation units).

There are two energy scales in the system determined by the extensional modulus of the filaments μ and the spring constant of the cross-linkers. To fix the energy scale in the problem we set the extensional modulus of the filaments to unity. The average spring constant for a filament segment can then be determined from the mean distance between cross-links, or, in other words, the network density: $\langle k_R\rangle=1/\langle l_c\rangle=150$. Physically, actin is a wormlike polymer, so the effective spring constant of each free length of polymer should be $k_R\sim k_BTl_p^2/l_c^4$ [8], where l_p is the persistence length of F-actin, which is approximately 17 μm [31]. Thus at room temperature, a 0.1 μm segment of actin will have $k_R\sim12$ pN/nm, while a 0.2 μm segment will have $k_R\sim0.7$ pN/nm. Because of the variability in this effective spring constant as a function of l_c, we choose to simulate a range of actin to cross-linker spring constant ratios. The measured unfolding force for an Ig domain is around 150 pN [32]—treating the cross-linker as a linear spring between unfolding events and using the sawtooth length given above, we arrive at a physiological spring constant of $k_f\sim8$ pN/nm. Thus the relevant dimensionless ratio of spring constants to study for physiological systems may lie in the range between $0.4<k_f/\langle k_R\rangle<7$. In simulation units, the range of cross-linker spring constant values reported here was between $10^1<k_f<10^4$, which corresponds to a range of spring constant ratios between $0.06<k_f/\langle k_R\rangle<66$.

A. Elastic moduli

Since we have omitted the bending rigidity of the filaments, these networks necessarily have vanishing elastic moduli in their unstrained state [34]. It has been shown that *in vitro* F-actin filamin networks do have a finite modulus at zero shear, though the differential modulus increases by a factor of 100 or more upon shearing [18]. Our networks quickly develop nonzero moduli under finite strain. To characterize the nonlinear mechanical properties of the network we measure the differential moduli $\partial\sigma_{ij}/\partial u_{ij}$ as a function of applied strain. Figure 2 shows how the differential shear modulus evolves as a function of strain. As expected, the differential moduli all vanish for zero applied strain. Upon increasing applied strain, they grow monotonically to some maximum where the network is stiffening most dramatically under further strain increments. At still larger values of the applied strain, the stress plateaus so that the differential moduli shown here decay to zero. In part (a) of Fig. 2 we show the differential shear modulus $K(u_{xy})$ for networks with $l_f/l_c=0.1$ as computed from the additional shear extension of the network already under shear u_{xy}. In part (b) of this figure we show the differential shear modulus $K(u_{xy})$ for networks with $l_f/l_c=0.02$. Though not shown, we also measure the uniaxial extension modulus $\bar{K}$ for the case $l_f/l_c=0.02$. From a comparison of the two measurements we determine the effective Poisson ratio ν as function of applied strain [35] using

$$\nu=\frac{1}{2}\frac{3\bar{K}-2K}{3\bar{K}+K}. \tag{5}$$

For intermediate deformations, where the network is strain stiffening, the scale of $\bar{K}$ is about four times that of K, so $\nu\approx0.38$.

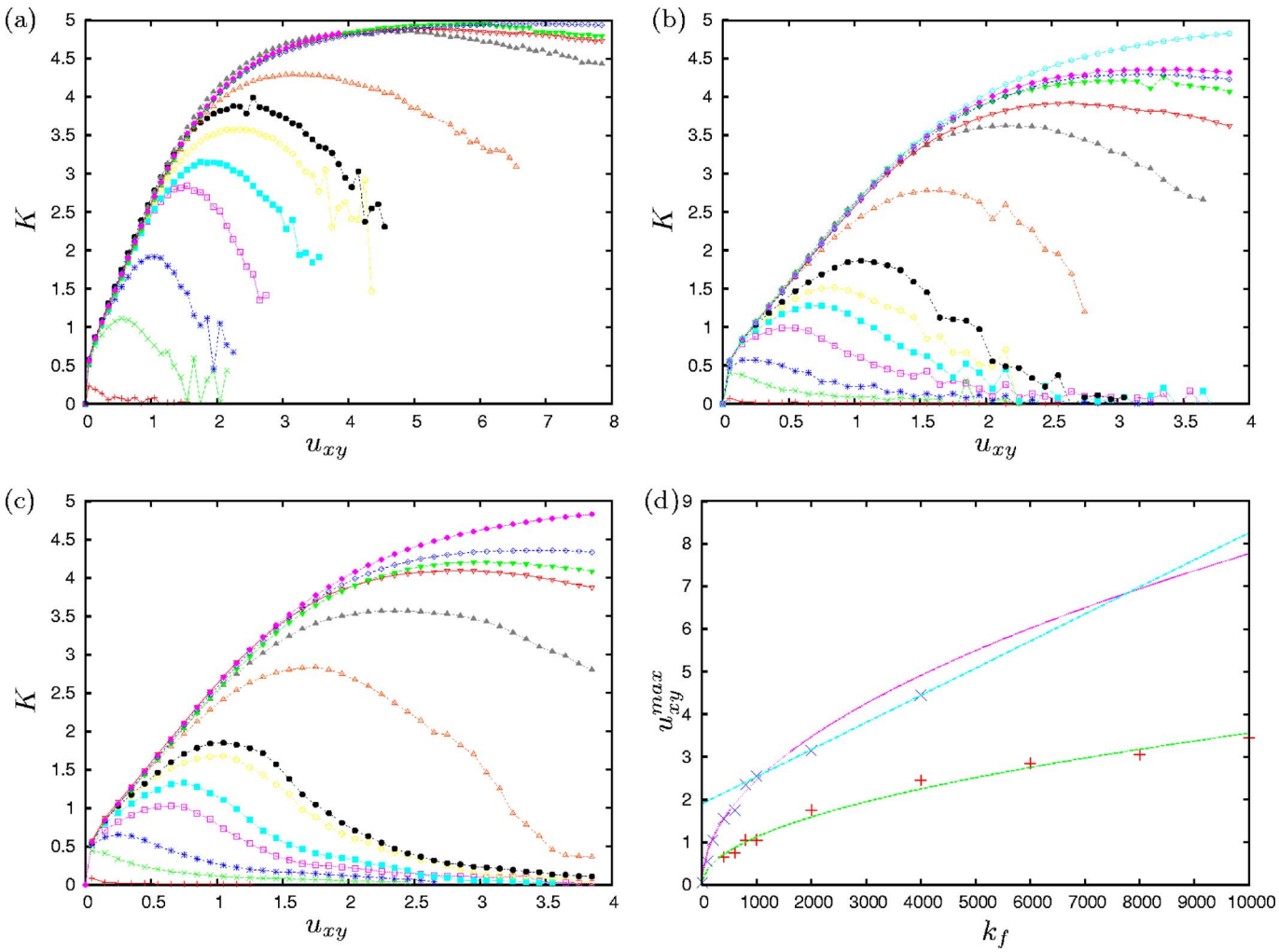

FIG. 2. (Color online) Differential moduli versus strain for several different cross-linker spring constants k_f. Modulus K is given in simulation units. (a) Shear modulus versus shear strain for $l_f/l_c=0.1$. (b) Shear modulus versus shear strain for $l_f/l_c=0.02$. (c) Shear modulus versus shear strain, for constant cross-linker force $f=k_f l_f$ with $l_f/l_c=0.02$. From lowest to highest curves in each graph, the cross-linker spring constants are, respectively 10, 100, 200, 400, 600, 800, 1000, 2000, 4000, 6000, 8000, 10000, and inextensible cross-links. (From Sec. IV, the average filament segment spring constant in these units is $\langle k_R \rangle \approx 150$.) (d) Strain value $u_{xy}^{\max}$ corresponding to the peak differential modulus from the data in (c) (lower points) and (a) (upper points) as a function of k_f. The curved lines are fits to $\sqrt{k_f}$. The straight line is a fit to $ax+b$ for values of $k_f \geqslant 1000$ and $l_f/l_c=0.1$.

The peak in the differential modulus was observed to coincide with the appearance of "tears" in the network. These tears were actually clusters of highly extended cross-linkers. Eventually, a single cluster of highly extended cross-linkers percolates across the network. Thus, the modulus peak occurs when a significant fraction of the cross-linkers are at their unfolding threshold.

The formation of the fragile state characterized by cross-linker unfolding requires a high-stress state. Since F-actin is found to rupture under tensile loads of 600 pN [33], one may ask whether F-actin rupture precludes the formation of the fragile state characterized by cross-linker unfolding. To check this we measured the tension along the actin filaments at the onset of cross-linker unfolding; we found that, although there are multiple cross-linkers connected to each filament, the force due to adjacent cross-linkers tend to cancel, so that stresses do not accumulate along the actin filaments. Using a conservatively high estimate unfolding force of filamin, 150 pN, we find that, at the onset of cross-linker unfolding, the stresses on individual segments of actin filament (between cross-links) were all below 4 times the cross-linker unfolding tension (600 pN), and 90% of filaments segments were at tensions below 3 times that value (450 pN). At larger strains these forces increase, and at strains 1.5 times the differential modulus peak, up to 20% of the actin filaments may be under more than 600 pN of tension, effectively breaking those strands. The breakdown of the network at large strains is safely above the region of interest in this work making the formation of the fragile state possible. Finally, we note that the unfolding tension of the cross-linker is actually an out-of-equilibrium quantity. At slower rates of tensile loading the cross-linkers will unfold typically at lower tensions due to thermally activated processes. Such thermal effects at lower loading rates, serve to widen the range of strain states in which cross-linker unfolding occurs

before F-actin failure. We will discuss the scaled tensions in the network further in Sec. V.

Since the tearing of the network corresponds to a segregation into actin-rich and cross-linker rich regions, we can thus approximate the compliance of the network as the compliance of a composite system. One part of the composite is the filament dominated parts of the network in which the cross-linkers are not greatly extended and the other part is the region of large cross-linker stretch. The effective modulus of the composite system can then be approximated as two nonlinear springs in series.

The force law for the filament dominated parts of the network can be inferred from the top curve in Fig. 2(b), which shows the differential shear modulus for networks with non-compliant cross-links. The shear modulus increases steadily at low shear as the individual filaments align with the shear direction. Above 200% strain, the modulus starts to plateau. In the limit of complete shear alignment, the extension of individual filaments is linear in the shear and thus the differential modulus is constant, with value $K(u_{xy})=n_{\mathrm{ave}}k_R$, where n_{ave} is the average number of filaments per unit cross sectional length. At low and intermediate values of the shear, the dependence of the modulus on absolute shear is complicated, reflecting simultaneous filament extension and alignment. In practice, we observe the growth of the modulus in this regime to be approximately linear in the shear.

In contrast, the part of the network dominated by highly extended cross-links can only sustain a finite maximum stress per unit area, since each cross-linker can only exert a maximum force of $k_f l_f$. In the limit of complete shear alignment, the maximum stress is given by

$$\sigma_{\max} = n_{\mathrm{cr}} k_f l_f, \tag{6}$$

where n_{cr} is the number of cross-linkers per unit of cross-sectional length that take part in the crazing, or splitting, of the network. n_{cr} is determined by the shortest percolation path across the network. We surmise that the differential modulus of the composite system reaches it maximum value at the onset of crazing. The expression above for the maximum stress implies that the onset of crazing is determined purely by the product $k_f l_f$. Indeed, Fig. 2(c) shows the modulus for sheared networks where the cross-linker force law is simply that given in Eq. (4): essentially a constant force cross-link with force $k_f l_f$. The curve is nearly identical to Fig. 2(b), for the sawtooth force law. A constant force law is by definition independent of network extension, so the differential modulus $\partial\sigma_{ij}/\partial u_{ij}$ is zero in a stretched, cross-linker dominated region of the network which has plateaued at the maximum stress $\sigma_{\max}$.

We now consider shear strain that maximizes the differential shear modulus. The maximum differential shear modulus occurs at the crossover point $u_{xy}^{\max}$, when the applied stress approaches $n_{\mathrm{cr}}k_f l_f$ as shown in Eq. (6). For smaller k_f/k_R, the crossover occurs in the linear growth region of the differential modulus, where $\sigma_{xy} \sim n_{\mathrm{ave}} k_R u_{xy}^2$, so the shear at maximum scales as $u_{xy}^{\max} \sim \sqrt{k_f/k_R}$. For larger k_f/k_R the crossover occurs in the region of constant differential shear modulus, so the shear at maximum scales as $u_{xy}^{\max} \sim k_f/k_R$. The plots in Fig. 2(d) shows $u_{xy}^{\max}$ versus k_f for the data in Figs. 2(a) and 2(b). The data for $l_f/l_c=0.02$ is consistent with $u_{xy}^{\max} \sim \sqrt{k_f}$. For $l_f/l_c=0.1$, the strain at maximum scales as $u_{xy}^{\max} \sim \sqrt{k_f}$ for $k_f \leqslant 1000$, then approaches a linear dependence on k_f at higher k_f.

For larger relative values of l_f the splitting of the network, and therefore the drop-off of the differential moduli, is suppressed at lower shear values. It does not occur until a finite fraction of the cross-linker population is stretched beyond its initial sawtooth length l_f. Still, in the limit of large strain, the modulus is mainly determined by the combination $F_{\max}=k_f l_f$. In the next section we will show that most stretched cross-linkers reach equilibrium near $F=F_{\max}$, so it is natural that the network elastic response is essentially that of a network with constant force cross-linkers.

In living cells, the action of molecular motors might lower the threshold of cross-link extension beyond the sawtooth length by prestressing the network. Indeed, it has been shown [18] that prestress is necessary to replicate physiological conditions in *in vitro* F-actin filamin systems. Physiologically, unfolding-based behavior should manifest itself once the average stress per filament exceeds the Ig domain unfolding stress of $\approx$150 pN [32]. For a dense network with 10 filaments per $\mu\mathrm{m}^2$ of cross section the critical prestress would amount to 1.5 kPa, while for sparse network with the order of 1 filament per $\mu\mathrm{m}^2$ the critical prestress would be 150 Pa or less.

B. Cross-linker extension statistics

The crazing or splitting of the network discussed in the last section occurs once the local strain forces experienced by cross-links exceeds $k_f l_f$, the maximum force sustainable by a cross-link sawtooth branch. We found that, in the subset of all cross-links which had been extended through at least one "unfolding event" (i.e., those cross-links which had changed sawtooth branches at least once), a characteristic distribution of equilibrium lengths (modulo l_f) emerges that is independent of total strain. Figure 3(a) shows the measured equilibrium distributions of cross-link lengths, modulo the sawtooth length l_f, for a representative set of strained networks with $l_f/l_c=0.1$ or $l_f/l_c=0.02$ and several values of spring constant k_f. For values of $k_f/\langle k_R\rangle < 10$ the statistical weight for finding a cross-link extension (modulo l_f) appears exponentially enhanced towards length l_f where the domains unbind. For values $k_f/\langle k_R\rangle > 10$ the statistical weight for finding a cross-link extension (modulo l_f) grows faster than exponentially near length l_f. For $k_f/\langle k_R\rangle \geqslant 4$ the distributions of cross-link lengths were identical for both measured values of l_f. At lower k_f there were significant differences between the $l_f/l_c=0.1$ and $l_f/l_c=0.02$ data, with the former showing a less pronounced pileup towards length l_f. The source of this deviation could be nonlinearities in the response of the softer networks over the longer length scale of $l_f/l_c=0.1$—our effective spring model assumed linear response.

According to the model developed in Sec. II, the cross-link length distribution is determined completely by the distribution of local effective network spring constants. In particular, there is nothing in Eq. (2) that would create an exponential in the length distribution unless that exponential

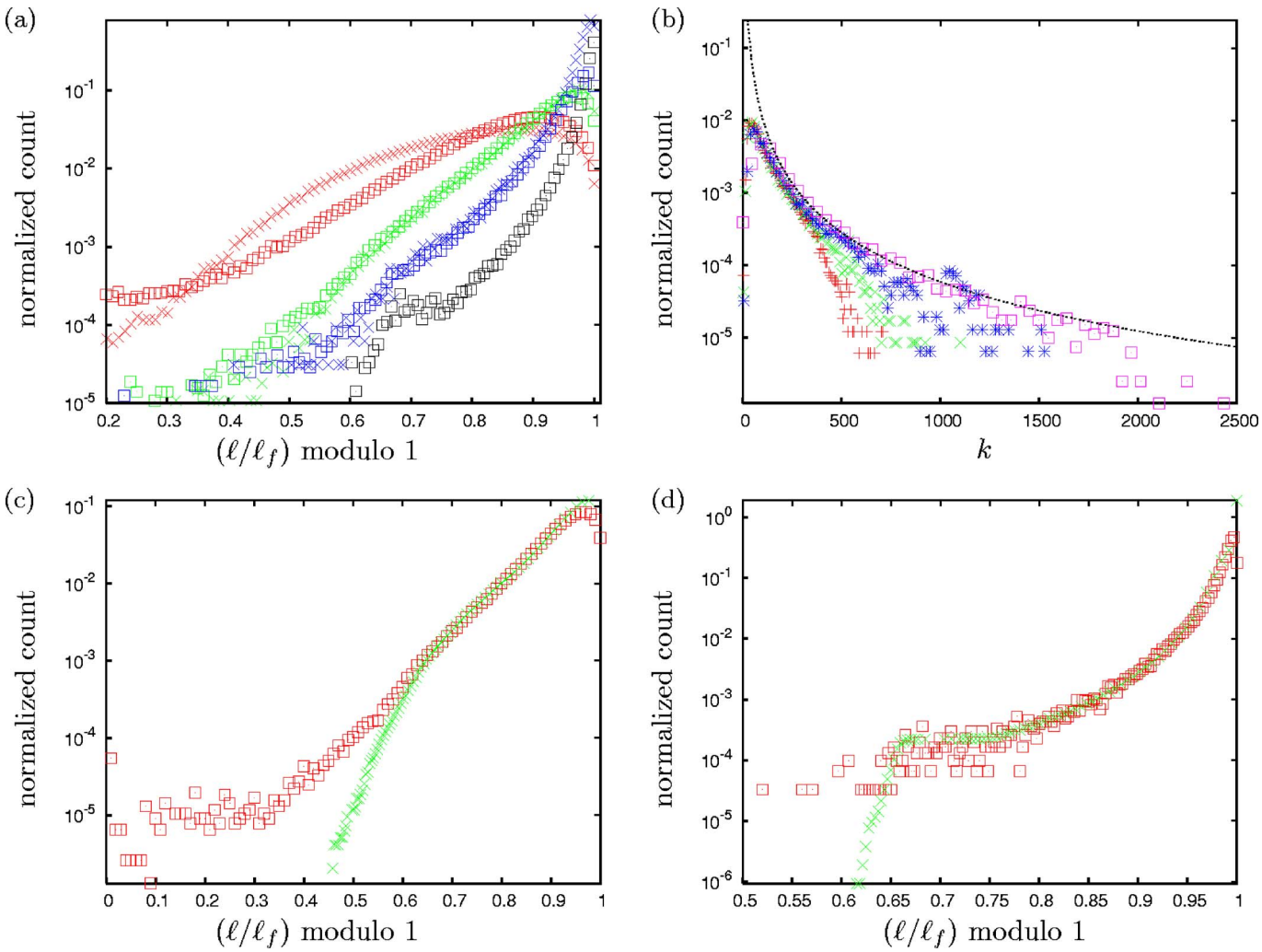

FIG. 3. (Color online) (a) Distribution of normalized cross-linker lengths l/l_f modulo 1 in equilibrated networks with, from shallowest to steepest slopes, respectively, k_f=100, 600, 2000, and 6000 (where $\langle k_R \rangle$=150). For the three smaller values of k_f, values were given for l_f/l_c=0.1 (crosses) and for l_f/l_c=0.02 (boxes). For k_f=6000 no significant pileup was measured for l_f/l_c=0.1. In plots (b)-(d) we only plot values for l_f/l_c=0.02. (b) Measured effective medium spring constant distributions for k_f=600, 1000, 2000, and 6000 (higher k_f have longer tails). The dashed line shows $k^{-2.25}$. (c) Distribution of normalized cross-linker lengths l/l_f modulo 1 for k_f=600 (boxes) compared to distribution predicted by Eq. (2) for the data in (b) (crosses). (d) Distribution of normalized cross-linker lengths l/l_f modulo 1 for k_f =6000 (boxes) compared to distribution predicted by Eq. (2) for the data in (b) (crosses).

were already contained in $P_K(k)$, the effective spring constant distribution function.

Figure 3(b) shows the measured distribution of effective network spring constants experienced by the cross-linkers sampled in Fig. 3(a). This distribution was found by probing one cross-link at a time, changing the force on the cross-link and numerically reminimizing over lattice displacements to find the corresponding change in length. We find that there is indeed a nontrivial and rapidly decaying distribution of effective spring constants. For high k_f the spring constant distribution approaches a power-law with exponent −2.25, while for lower k_f the distribution is truncated at high effective k, becoming nearly exponential.

We may use Eq. (2) to calculate $P(x_f)$, the expected distribution of cross-linker lengths modulo l_f, for the cases of exponential or power law $P_K(k)$. For the power law case with $P_K(k) \sim k^{-p}$, Eq. (2) yields a cross-link length distribution of the form

$$P(x_f) \simeq \frac{k_f^{1-p}}{p(p-1)l_f}\left[(p-1)\left(\frac{x_f}{l_f - x_f}\right)^p + p\left(\frac{x_f}{l_f - x_f}\right)^{p-1}\right]. \tag{7}$$

This form for $P(x_f)$ diverges at l_f for any $p>0$. Alternately, if the effective spring constants were exponentially distributed, with form $P_K(k) \sim e^{-k/\bar{k}}$, then $P(x_f)$ would take the form

$$P(x_f) \simeq \frac{\bar{k}}{l_f}\exp\left(\frac{k_f(x_f - l_f)}{\bar{k}x_f}\right) + \frac{k_f}{l_f}\Gamma\left(0, \frac{k_f(l_f - x_f)}{\bar{k}x_f}\right), \tag{8}$$

where the constant $\bar{k}$ is an undetermined material parameter and Γ is the incomplete gamma function. This expression grows exponentially near $x_f = l_f$.

Eqs. (7) and (8), together with the data in Fig. 3(b), are consistent with our observation that the cross-linker length

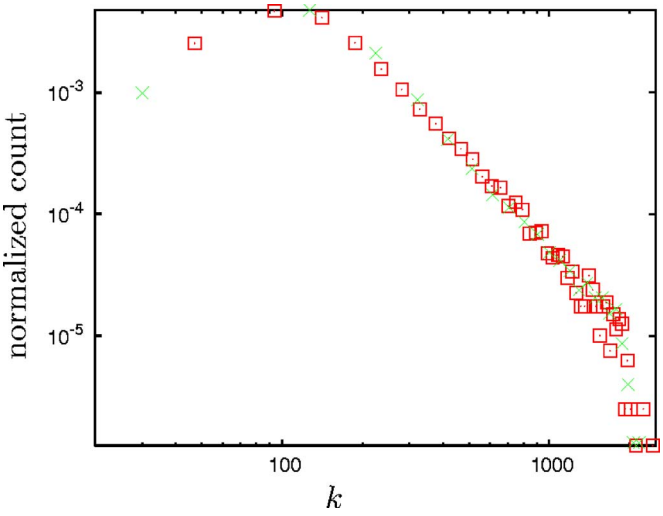

FIG. 4. (Color online) Measured effective medium spring constant distributions for $k_f/\langle k_R\rangle=40$. Box points are for a network with sawtooth cross-linkers, while the cross points are for a network with linear spring cross-links. Plots for $l_f/l_c=0.02$.

distribution grows exponentially for low k_f and even faster for high k_f, since the respective forms for $P_K(k)$ for these two cases are exponential and power law. Figure 3(c) shows the result of numerically evaluating Eq. (2) on the data from Fig. 3(b) for $k_f/\langle k_R\rangle=4$. The agreement between the theoretical prediction for $P(x_f)$ and the actual measured distribution is very good at high x_f. Similarly, Fig. 3(d) shows the result of numerically evaluating Eq. (2) for the measured $P_K(k)$ for $k_f/\langle k_R\rangle=40$. The agreement between theoretical prediction and measurement is outstanding.

Figure 4 again shows $P_K(k)$ for $k_f/\langle k_R\rangle=40$. The distribution function for sawtooth force law cross-linkers is compared to the distribution for a network which was created and equilibrated under strain with linear force law cross-linkers. Both distributions are identical, demonstrating that the presence of the sawtooth force law does not determine the distribution of $P_K(k)$. This justifies our use of a mean-field approach in Sec. II, since $P_K(k)$ is not influenced by $P(x_f)$. The further implication is that the origin of the measured $P_K(k)$ is purely geometrical.

We have seen that for large values of the sawtooth spring constant k_f the local spring constant distribution in the random network has a power law decay in the large k regime as shown by the boxed points in Fig. 3(b). These points are fit by the dashed line representing a power law with exponent $-9/4$. The power law behavior is also clearly visible in the log-log plot in Fig. 4, which shows the higher k_f data with $l_f/l_c=0.02$. For smaller values of k_f, e.g., the crosses in the Fig. 3(b), the local spring constant distribution exhibits a clearly exponential decay. Considering the full set of the numerical data shown in Fig. 3(b) for varying values of k_f ranging (in simulation units) from 600 to 6000, we note the following trends. First, the distribution appears to transition from a power law form at higher k in the case of stiffer cross-linker springs, i.e., larger values of k_f, to an exponential form for softer cross-linker springs. Secondly, the maximum values of local spring constants observed in the system appear to be generically smaller than the cross-linker spring constant for that system. Finally, each data set for a given k_f appears to follow the power law decay for smaller values of k before reaching an exponentially decaying terminal regime at the largest measured values of k.

We now speculate as to the origin of these phenomena beginning with an examination of the power lay decay seen for smaller values of k in all the data sets. Since this effect is more robust at larger values of the cross-linker spring constants, consider first the limiting case of perfectly incompliant cross-linkers. Here the local effective spring constant of the network must be completely determined by the filaments, and, in particular, by the distribution of filament lengths between cross-links. The distances between cross-links l_c for a random network such as ours are exponentially distributed, with

$$P(l_c)dl_c \sim e^{-l_c/\langle l_c\rangle}dl_c. \tag{9}$$

as shown by Kallmes and Corte [36]. Since the spring constant of each filament segment is proportional to $1/l_c$, the probability of the occurrence of a filament segment spring constant between k and $k+dk$ takes the form

$$P(k)dk \sim e^{-1/(\langle l_c\rangle k)}k^{-2}dk. \tag{10}$$

Furthermore, if we assume that softer regions of the network from which the smaller values of local spring constant k are measured form small pockets in a material that is generally less compliant, then it is reasonable to suppose that the deformation imposed on the network due to the external forces applied in those softer regions will lead to a highly localized deformation involving only a few network springs. Then the local effective spring constant around those cross-links is determined primarily by a few filament segments whose effective spring constants statistics will be governed by Eq. (10). For large values of k, this expression approaches k^{-2}, which is consistent with our findings for large k_f. The exponential in Eq. (10) becomes unimportant for $1 \lesssim \langle l_c\rangle k$ so that for $150 \lesssim k$ we expect to see a only power law distribution of local spring constants with an exponent of -2.

The effective spring constant of any two springs in series is less than the spring constant of either of them. Since all filaments are connected to one another through cross-linkers with spring constant k_f, it is clear that this power law tail in Eq. (10) cannot extend to values of k greater than k_f. If we consider the large-k tail of the spring constant distribution, we must look at rarely found regions in the network that lie on chains of anomalously stiff network springs corresponding to very short network filaments. Each of these chains of springs is made up of a number of statistically independent springs connected in series. In order to find an extremely large value of the effective spring constant k it must be that for one of the force paths all of the constituent spring constants are large, since the compliance of the springs in series will be dominated by any single soft spring. We expect the probability of such a rare event to be Poisson distributed so that, in the high-k tail, the distribution $P_K(k)$ takes the form

$$P_K(k) \sim H(k)e^{-k/\bar{k}}, \tag{11}$$

where H is some regular function characterizing the small-k behavior of the distribution [$H(x) \to \text{const}$ as $x \to \infty$] discussed above and the constant $\bar{k}$ is undetermined by this heuristic argument. Such an exponential distribution is consistent with the data for low k_f presented in Fig. 3(b).

Interestingly, we do indeed see that each distribution has an exponential tail for values of k approaching an upper limiting value of k_f. The value of this upper limit appears to be $\propto k_f$ with a coefficient of proportionality of order unity. This suggests that if the stiff chains of springs associated with the stiffest region of the material contains of order n springs in series then there must be of order n such chains in parallel to account for the upper limit.

The principal effect of changing k_f on the elasticity of the random network is to push the cross-over from a power law decay to the exponential tail to larger values of k. We have presented arguments for both this lower-k power law and higher-k exponential dependence of the local spring constant distribution. We cannot account for approximately 10% discrepancy between the measured and predicted exponents for the power law and we cannot estimate using these arguments the cross-over value of k between these two behaviors. Nevertheless we see, regardless of the form of the local spring constant distribution, (2) accurately relates that distribution to the cross-linker extension distribution as shown by Figs. 3(c) and 3(d).

V. DISCUSSION

In this work we have studied a composite network of linear elastic elements having randomly distributed spring constants cross-linked by linkers that have the sawtooth force-extension relation common to proteins with repeated unfolding domains. While this system is clearly an oversimplification of both the chemical complexity and semiflexible character of the cytoskeleton, these networks retain one important microarchitectural feature of the F-actin networks in that forces must propagate from filament to filament through a linking molecule exhibiting a highly nonlinear (sawtooth) force response to strain. We suspect that our model system can thus inform the understanding of the mechanical properties of physiological cytoskeletal networks, which are the subject of recent theoretical work and are being probed experimentally with increasing quantitative accuracy [23,37,38].

Our most striking result is the observation of the development of a highly fragile mechanical state in the network at large strains. At moderate strain, a nontrivial number of cross-linking molecules reach a critical state where they are poised to unfold another domain. The presence of fluctuating internal stresses in the cytoskeleton produced by variations in molecular motor activity and/or thermally generated fluctuations can act on this highly fragile state to produce strain fluctuations at all frequency scales, due to the broad distribution of local energy wells in the system. Thus, the formation of this critical state under applied stress may explain a particular feature of the low-frequency strain fluctuations as observed by intracellular microrheology.

The inclusion of sawtooth cross-linkers in the analysis of the mechanics of semiflexible networks may explain some features of the nonlinear elasticity of the cytoskeleton. It is well known that *in vitro* F-actin networks when cross-linked by rigid, inextensible molecules generically show strain hardening [16] at least at network densities consistent with the affine response regime [12]. We did not include the nonlinearity of the longitudinal compliance of the actin filaments, which accounts for this strain hardening. The mechanics of unfolding cross-linkers presents an additional nonlinear effect that decreases the differential modulus. Taking both effects into account, we expect that highly strained F-actin/filamin gels to strain harden *less than* than that predicted by Ref. [8] and eventually show a strain softening regime at high strains.

While strain hardening is a hallmark of highly cross-linked semiflexible networks, the *in vivo* cytoskeleton has been seen to strain soften [39]. Based on this work we suggest that strain softening in densely cross-linked semiflexible networks may be the result of the unfolding of specialized cross-linking proteins in it. From our numerical data it is clear that cross-linking of these networks by unfolding linkers can generate a strain softening material at large enough stresses so that domain unfolding occurs. It remains to be seen how or whether the interaction of these cross-linkers with motor proteins shifts this nonlinear elastic regime to lower applied strains.

We believe that this work suggests the appropriate theoretical framework for understanding the underlying mechanism by which the system reaches this highly fragile state. We note, however, that much remains to be done in order to develop this understanding into a theory that makes quantitatively accurate predictions. In addition it is clear that more precise numerical explorations of the network are required in order to better characterize both the local elastic constant distribution in the network as well as the cross-linker length distribution. Nevertheless, it appears that the creation of this fragile state is a robust phenomenon.

In addition, recent experiments by the Janmey group report that rigidly cross-linked semiflexible networks generically show a large, negative first normal stress coefficient [40]. We know of no such measurements on the *in vivo* cytoskeleton. Noting that sawtooth cross-linking of these networks changes their nonlinear elasticity, we believe it will be important to study the effect of unfolding cross-linkers on this nonlinear elastic response as well.

There are a number of other extensions of this work that remain to be considered. We are currently working to add thermalized subcritical unfolding, along with energy input through the action of simulated molecular motors. The nonequilibrium steady state thus established will be closer to the conditions inside cells. The strain rate dependent unfolding force [30] then depends on the frequency spectrum of molecular motor activity, so that the effective unfolding threshold, and thus all other forces in the network, may be shifted down by a factor of 2 or more. The development of a more complete model that includes the effect of internally generated random stresses due to the action of molecular motors

will be an important step towards the direct calculation of the low-frequency dynamics of this biopolymer gel of fundamental biological importance.

ACKNOWLEDGMENTS

B.D. and A.J.L. thank J.C. Crocker for providing unpublished data and for enjoyable discussions. B.D. also thanks David Morse for enlightening discussions. A.J.L. was supported in part by Grant No. NSF-DMR0354113. B.D. acknowledges the hospitality of the UCLA department of Chemistry and the California Nanoscience Institute where part of this work was done. B.D. also acknowledges partial support from Grant No. NSF-DMR0354113 and the Institute for Mathematics and its Applications with funds provided by the National Science Foundation.

[1] B. Alberts, D. Bray, J. Lewis, M. Raff, K. Roberts, and J. D. Watson, *Molecular Biology of the Cell*, 3rd ed. (Garland, New York, 1994); P. A. Janmey, Curr. Opin. Cell Biol. **3**, 4 (1991).
[2] T. D. Pollard and J. A. Cooper, Annu. Rev. Biochem. **55**, 987 (1986).
[3] E. L. Elson, Annu. Rev. Biochem. **17**, 397 (1988).
[4] M. Rubenstein and R. H. Colby, *Polymer Physics* (Oxford University Press, London, 2003).
[5] P. A. Janmey, S. Hvidt, J. Lamb, and T. P. Stossel, Nature (London) **345**, 89 (1990).
[6] K. Kroy and E. Frey, Phys. Rev. Lett. **77**, 306 (1996).
[7] R. Satcher and C. Dewey, Biophys. J. **71**, 109 (1996).
[8] F. C. MacKintosh, J. Käs, and P. A. Janmey, Phys. Rev. Lett. **75**, 4425 (1995).
[9] D. A. Head, A. J. Levine, and F. C. MacKintosh, Phys. Rev. Lett. **91**, 108102 (2003).
[10] J. Wilhelm and E. Frey, Phys. Rev. Lett. **91**, 108103 (2003).
[11] D. A. Head, F. C. MacKintosh, and A. J. Levine, Phys. Rev. E **68**, 025101(R) (2003).
[12] D. A. Head, A. J. Levine, and F. C. MacKintosh, Phys. Rev. E **68**, 061907 (2003).
[13] Alex J. Levine, D. A. Head, and F. C. MacKintosh, J. Phys.: Condens. Matter **16**, S2079 (2004).
[14] B. A. DiDonna and T. C. Lubensky, Phys. Rev. E **72**, 066619 (2005).
[15] D. A. Head, A. J. Levine, and F. C. MacKintosh, Phys. Rev. E **72**, 061914 (2005).
[16] M. L. Gardel, J. H. Shin, F. C. MacKintosh, L. Mahadevan, P. Matsudaira, and D. A. Weitz, Science **304**, 1301 (2004).
[17] P. R. Onck, T. Koeman, T. van Dillen, and E. van der Giessen, Phys. Rev. Lett. **95**, 178102 (2005).
[18] M. L. Gardel, F. Nakamura, J. H. Hartwig, J. C. Crocker, T. P. Stossel, and D. A. Weitz, Proc. Natl. Acad. Sci. U.S.A. **103**, 1762 (2006).
[19] S. Labeit and B. Kolmerer, Science **270**, 236 (1995).
[20] M. Rief, M. Gautel, F. Oesterhelt, J. M. Fernandez, and H. E. Gaub, Science **276**, 1109 (1997).
[21] I. Schwaiger, A. Kardinal, M. Schleicher, A. A. Noegel, and M. Reif, Nat. Struct. Mol. Biol. **11**, 81 (2004).
[22] D. J. Brockwell, G. S. Beddard, E. Paci, D. K. West, P. D. Olmsted, D. A. Smith, and S. E. Radford, Biophys. J. **89**, 506 (2005).
[23] B. D. Hoffman, K. A. Miranda, G. Massiera, and J. C. Crocker, Biophys. J. **88**(1), 493A (2005).
[24] M. F. Coughlin, M. Puig-de-Morales, P. Bursac, M. Mellema, E. Millet, and J. J. Fredberg, Biophys. J. **90**, 2199 (2006).
[25] B. Fabry, G. N. Maksym, J. P. Butler, M. Glogauer, D. Navajas, and J. J. Fredberg, Phys. Rev. Lett. **87**, 148102 (2001).
[26] R. E. Laudadio, E. J. Millet, B. Fabry, S. S. An, J. P. Butler, and J. J. Fredberg, Am. J. Physiol.: Cell Physiol. **289**, C1388 (2005).
[27] P. Bursac, G. Lenormand, B. Fabry, M. Oliver, D. A. Weitz, V. Viasnoff, J. P. Butler, and J. J. Fredberg, Nat. Mater. **4**, 557 (2005).
[28] P. Sollich, Phys. Rev. E **58**, 738 (1998).
[29] B. A. DiDonna and Alex J. Levine, Phys. Rev. Lett. **97**, 068104 (2006).
[30] E. Evans and K. Ritchie, Biophys. J. **72**, 1541 (1997).
[31] E. Frey, K. Kroy, and J. Wilhelm, in *Dynamical Networks in Physics and Biology*, edited by D. Beysens and G. Forgacs (EDP Sciences Springer, Berlin, 1998).
[32] Furuike, S., T. Ito, and M. Yamazaki, FEBS Lett. **498**, 72 (2001).
[33] Y. Tsuda, H. Yasutake, A. Ishijima, and T. Yanagida, Proc. Natl. Acad. Sci. U.S.A. **93**, 12937, (1996).
[34] M. Kellomäki, J. Åström, and J. Timonen, Phys. Rev. Lett. **77**, 2730 (1996).
[35] L. D. Landau and E. M. Lifshitz, *Theory of Elasticity*, 3rd ed. (Pergamon Press, Oxford, 1986).
[36] O. Kallmes and H. Corte, Tappi J. **43**, 737 (1960).
[37] A. W. C. Lau, B. D. Hoffman, A. Davies, J. C. Crocker, and T. C. Lubensky, Phys. Rev. Lett. **91**, 198101 (2003).
[38] L. Deng, X. Trepat, J. P. Butler, E. Millet, K. G. Morgan, D. A. Weitz, and J. J. Fredberg, Nat. Mater. **5**, 636 (2006).
[39] J. J. Fredberg, (private communication).
[40] F. C. MacKintosh and P. A. Janmey, (private communication).